Effect of surface stabilization of nanoparticles on luminescent characteristics in ZnO/poly(hydroxyethyl methacrylate) nanohybrid films

Chin-Hsien Hung and Wha-Tzong Whang*

Received 13th April 2004, Accepted 12th August 2004
First published as an Advance Article on the web 16th September 2004
DOI: 10.1039/b405497k

Highly transparent and stable luminescent ZnO/poly(hydroxyethyl methacrylate) nanocomposites have been synthesized *via* a nanoparticle surface modified method. 3-(Trimethoxysilyl)propyl methacrylate (TPM) was used as the stabilizing agent in a simple, mild sol–gel route to prepare TPM-modified ZnO nanoparticles. The existence of TPM on the nanoparticle surface effectively promotes the stability of colloidal ZnO nanoparticles and the compatibility between the inorganic nanoparticles and the organic matrix in the solid nanohybrid. The resulting ZnO/PHEMA nanocomposites with TPM-modified nanoparticles have better dispersibility and controllable luminescent properties. The characteristics of TPM-modified and unmodified ZnO nanoparticles have been studied by ultraviolet-visible (UV-vis) absorption spectroscopy, powder X-ray diffraction (XRD), transmission electron microscopy (TEM), Fourier transform infrared (FTIR) and ^{1}H NMR spectroscopy.

Introduction

Nanoparticles (NPs) or nanocrystals (NCs) of semiconductor materials have been extensively studied in the last decade for use in light emitting diodes, lasers, photovoltaic solar cells and biolabels.[1–6] Many research groups have focused on the superior emitting properties of nanocomposites by dispersing the quantum-sized particles into a polymeric matrix.[7–11] The hybrid nanocomposites not only inherit the high luminescence of the quantum dots but also possess advantages of polymers such as flexibility, film integrity, and conformity. The control of the particle size, size distribution and dispersion homogeneity over the entire matrix is the critical prerequisite to assure the optical and electrical properties of the nanocomposites for nanodevice applications. Up to now, to hybridize the inherently hydrophilic inorganic nanoparticles into a polymer matrix *via* bulk polymerization of an organic monomer is still a technological challenge.[12,13] Generally, passivating nanoparticle surfaces with appropriate capping agents such as long-chain aliphatic thiols[14,15] or amines[8] is the most efficient method to prevent aggregation of the innately unstable nanoparticles and thus enhance the compatibility of the inorganic nanoparticles with the organic matrix.

Among metal oxide materials, zinc oxide (ZnO) with its wide band gap (3.4 eV) and large exciton binding energy (60 meV) has been of particular interest for catalysts, sensors and optoelectronic devices.[16–18] Since the luminescence characteristics of ZnO quantum dots are size-dependent,[19–23] so the size control is quite important. The strategies to control the particle sizes include encapsulating an organic capping agent on the nanoparticle surfaces such as alkylthiols, polymer micelles,[24,25] or using coordinating solvent such as dimethyl sulfoxide, *N*,*N*′-dimethylformamide and tri-n-octylphosphine oxide.[26–29] Although the size of nanoparticles can be manipulated by the capping agents,[24,25] the nanoparticles under ambient conditions still will gradually and irreversibly aggregate together, especially when the solvent is evaporated. More importantly, the aggregated nanoparticles cause serious drawbacks in the photoluminescence, in terms of wavelength shift and intensity decay.[19,20] Recently, stable-luminescent powder-like ZnO/SiO_2 hybrids prepared by spray drying of SiO_2 and ZnO nanoparticles colloids at 200 °C were reported.[30] In addition, Okuyama[31] *et al.* described the preparation of tunable emission ZnO nanocomposites *via* the incorporation of different sizes of particles in the presence of poly(ethylene glycol) solutions. However, the long term stability of nanoparticles in both solution and bulk polymers is still an unsolved problem. In this article, we intend to modify the ZnO nanoparticle surfaces to promote the stability of colloid suspensions and nanocomposites, thus preserving the luminescent properties of nanoparticles in the nanohybrid bulk. We prepared a series of stabilized quantum size ZnO with various particle sizes, and chemically hybridized the nanoparticles into bulk polymers. The surface of the nanoparticles was stabilized by the absorption and hydrolysis of an unsaturated aliphatic silane, 3-(trimethoxysilyl)propyl methacrylate (TPM), *via* a mild sol–gel reaction. The colloidal ZnO nanoparticles were first dispersed in 2-hydroxyethyl methacrylate (HEMA) monomers and then thermally polymerized to form a stable nanohybrid film. Besides, the unsaturated chain of TPM on the ZnO nanoparticles can be polymerized with 2-hydroxyethyl methacrylate, making the particles uniformly dispersed in the poly(2-hydroxyethyl methacrylate) (PHEMA) matrix (Scheme 1). With this approach, we have prepared a series of highly transparent nanocomposites with uniform and well-defined size of ZnO nanoparticles. The colloidal ZnO nanoparticles and the nanoparticle/polymer composites were also characterized with X-ray diffraction (XRD), Fourier transform infrared (FTIR), transmission electron microscopy (TEM), UV-vis absorbance and

*wtwhang@mail.nctu.edu.tw

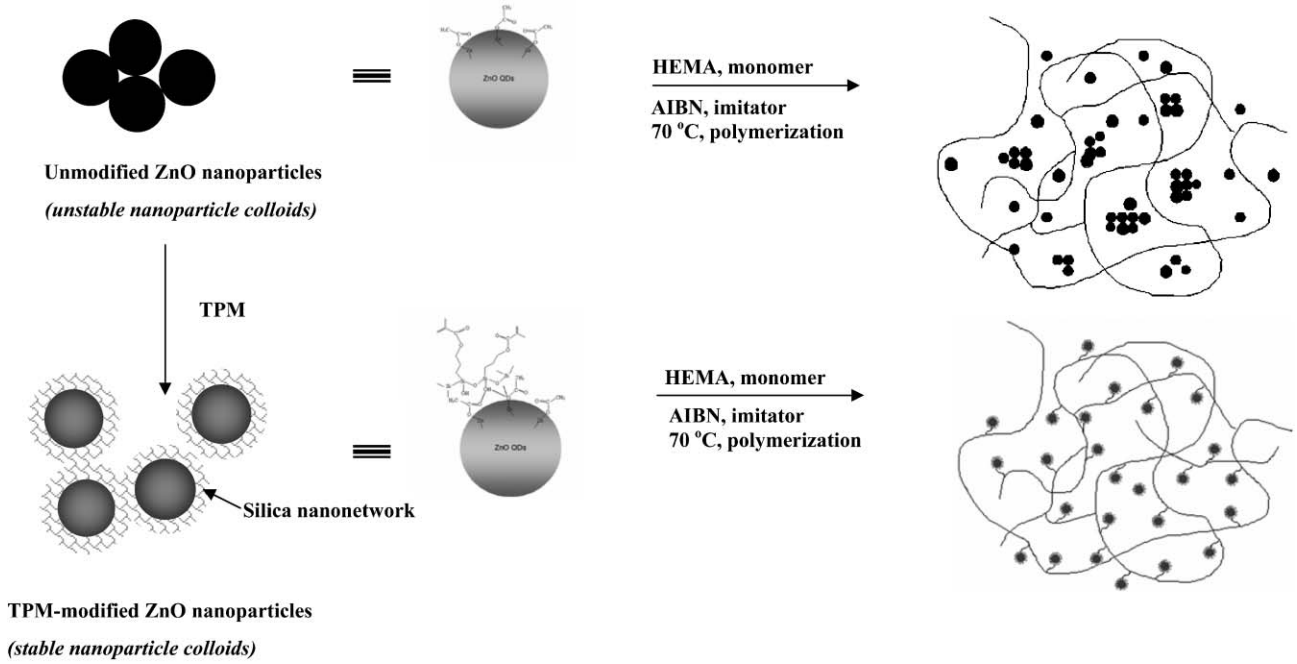

Scheme 1 The synthesis procedure of ZnO/PHEMA nanocomposites.

photoluminescence spectroscopy (PL), Fourier transform infrared (FTIR) and ^{1}H NMR spectroscopy.

Experimental

Materials

Zinc acetate dihydrate ($Zn(Ac)_2 \cdot H_2O$) (SHOWA, 99.0%), lithium hydroxide monohydrate ($LiOH \cdot H_2O$) (TEDIA, 99.0%), 3-(trimethoxysilyl)propyl methacrylate (TPM) (Aldrich, 98.0%) and absolute ethanol (Nasa, 99.5%,) were used as received. 2-Hydroxyethyl methacrylate (HEMA, 97.0%) and methyl methacrylate (MMA, 99.0%) from Acros were distilled under vacuum before use. 2,2′-Azobisisobutyronitrile (AIBN, 99.0%) from SHOWA was recrystallized from methanol.

Synthesis of ZnO nanoparticles

Green-emitting ZnO nanoparticles with an average diameter of 3.2 nm were prepared following the previous reports[18] with minor modification. In a typical run, 3.29 g of $Zn(Ac)_2 \cdot H_2O$ was dissolved in 150 mL boiling ethanol then refluxed at 80 °C in a nitrogen atmosphere, and held at this temperature for 3 h under vigorous stirring. To end this process, 90 mL of ethanol was removed by distillation and the solution was subsequently diluted to the original volume by adding the same amount of fresh ethanol. The reaction mixture was then cooled to 0 °C. A 90 mL aliquot of 0.87g $LiOH \cdot H_2O$ in ethanol was dropped into the stock solution under constant stirring within 2 h; several hours of stirring with sonication assistance were needed to completely dissolve $LiOH \cdot H_2O$ in the ethanol. The stock solution was then stirred continuously at room temperature for 2 h until the ZnO nanoparticle colloids became transparent. Finally, the nanoparticle solution was filtered through a 0.1 μm glass fiber filter to remove any insoluble precipitates. Blue-emitting nanoparticles with an average diameter of 2.2 nm were synthesized in a similar way, except the molar ratio of LiOH : $Zn(Ac)_2 \cdot H_2O$ was raised to about 3.5.[31] In addition, orange-emitting ZnO nanoparticles (6.1 nm diameter) were synthesized according to the method developed by Hoyer *et al.*[32]

Synthesis of TPM-modified ZnO nanoparticles

To stabilize the surface of ZnO nanoparticle colloids, 0.3 g TPM in 10 ml ethanol was injected into 200 ml of as-prepared ZnO nanoparticle colloids over about 1 hour at 0 °C. The mixture was then further stirred at room temperature for 12 h followed by filtration with a 0.1 μm glass fiber filter to remove any insoluble precipitates.

Preparation of nanoparticle powder

To obtain the ZnO nanopowder for characterization, the ZnO nanoparticle colloids (unmodified and TPM-modified samples) were precipitated by adding a excess of anti-solvent such as hexane or heptane into the ethanol solution (volume ratio: heptane/ethanol > 2),[33] called a "washing process". Briefly, 100 ml nanoparticle solution was poured into 300 ml heptane to cause nanoparticle precipitation. The resulting precipitates were isolated by centrifugation, decantation and rewashing several times to remove all residue. The resulting product was then collected and dried under vacuum. The amount of TPM stabilizing agent absorbed on the ZnO nanoparticle surface can be estimated by TGA analysis and was found to be about 4.3 wt%.

Preparation of ZnO nanocomposites

Unmodified and TPM-modified ZnO nanoparticles colloids were first purified through "washing process" and redispersed

in 250 ml of fresh ethanol. Then, 5 ml of nanoparticle colloids (ZnO content of ~1 wt%) were mixed with 10 g HEMA monomer under stirring at room temperature for 2h. Ethanol solvent was distilled by using a rotatory evaporation at about 40 °C. To polymerize ZnO NPs-monomers, 0.2 wt% AIBN radical initiator was added into the precursor solution. The mixture was then gently stirred for several hours until the solution became clear. Finally, the ZnO nanoparticles/polymer hybrid materials were obtained by pouring the solution in a Teflon mold (30 mm diameter × 3mm height) by subsequently bulk polymerization in an oven at 70 °C for 6 h, and further postheating at 100 °C for 2 h after being removed from the mold.

Characterization

All measurements for characterization were performed at room temperature. X-Ray powder diffraction patterns were recorded with a MAC Science MXP18 X-ray diffractometer (30 kV, 20 mA) with copper targets at a scanning rate of 4° min^{-1}. The Fourier transform infrared (FTIR) spectra of the samples were obtained with a Nicolet PROTÉGÉ-460 by the KBr method. ^1H NMR spectra were recorded on a Varian Unity-300 NMR spectrometer. Thermal gravimetric analyses of the ZnO nanoparticles were carried out with a Du Pont TGA 2950 at a heating rate of 10 °C min^{-1} with a nitrogen purge. UV-vis absorbance spectra were recorded on an Aligent 8453 spectrometer using a 1 cm quartz cuvette. Transmission electron microscopy (TEM) was carried out on a JEOL 2000FX electron microscope operating at 200 kV. The nanoparticle samples were prepared by directly placing a drop of solution on a holey copper grid covered with a continuous carbon film. The specimens of nanocomposites were ultra-microtomed with a diamond knife on a Leica ultracut Uct to obtain about 100 nm thick films. Subsequently, these films were placed on a 200 mesh copper net and a layer of carbon about 3 nm thick was deposited for TEM observation. The photoluminescence properties of ZnO nanoparticle solutions and nanocomposites were measured on a Hitchai F4500 fluorescence spectrometer equipped with an excitation source of 325 nm wavelength. The PL quantum efficiencies of ZnO nanoparticle colloids were measured by using quinine dye in H_2SO_4 aqueous solution as a PL reference.[34]

Results and discussion

Stability of ZnO nanoparticle colloids

Fig. 1 shows the TEM image of fresh unmodified ZnO nanoparticles dispersed in ethanol. The TEM image reveals spherical particles and the average diameter was estimated as about 3.2 nm. The size distribution histogram in Fig. 1 suggests a nearly uniform size distribution. Fig. 2 illustrates UV-vis absorption spectra of unmodified ZnO nanoparticles and TPM-modified ZnO nanoparticles in ethanol solution. The UV-vis absorption spectra of the two colloidal solutions which were recorded after 2 h aging reveal a well-defined exciton band at around 320 nm and a dramatic blue shift compared with the bulk excition absorption (373 nm).[35] Such features in the exciton band are mainly responsible for the

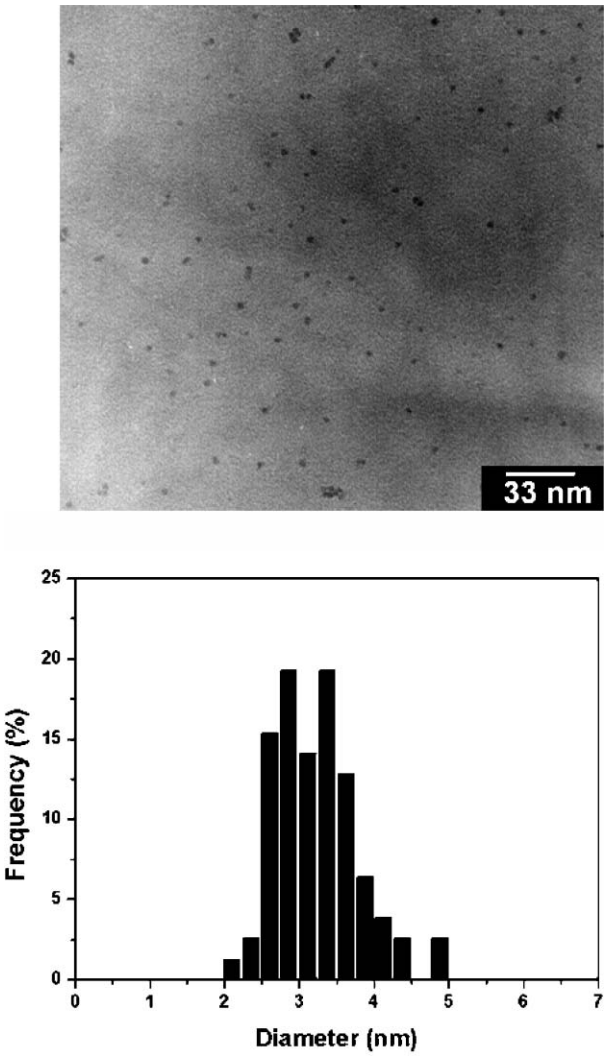

Fig. 1 TEM image and size distribution histogram of fresh unmodified ZnO particles.

characteristics of quantum size effects (particle size ⩽ 7 nm).[36] Generally, the fresh ZnO nanoparticles prepared from zinc acetate dihydrate in ethanol solution can be electrostatically stabilized by negatively-charged repulsion between carboxylic acid groups on the nanoparticle surfaces.[21] However, as the aging times were prolonged, the absorption shoulder of unmodified ZnO nanoparticles obviously undergoes a series of red-shifts (Fig. 2a), which mainly result from the development of some degree of aggregation between primary clusters.[19] Moreover, the aggregated clusters were accompanied with the formation of turbid suspensions in the solution. As shown in the inset of Fig. 2a, the ZnO nanoparticle settled to the bottom of the UV cell about two months later at room temperature. In contrast, the profiles in the absorption spectra of TPM-modified ZnO nanoparticles recorded at different aging times are almost identical (Fig. 2b). The solution with TPM-modified ZnO nanoparticles remains optically clear at room temperature during 2 months storage (inset in Fig. 2b) and remains stable for at least six months without any obvious colloidal aggregation. The stabilities of the TPM-modified

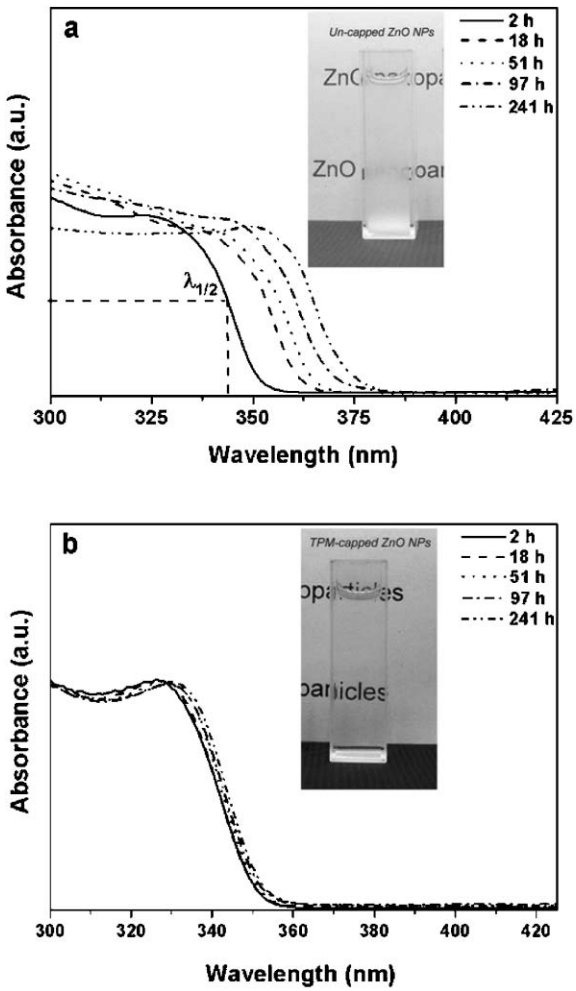

Fig. 2 Time dependence of UV-vis absorption spectra: (a) unmodified ZnO nanoparticles and (b) TPM-modified ZnO nanoparticles in ethanol. Inset are photographs of the ZnO nanoparticle colloids after aging at room temperature for 2 months.

ZnO particles are excellent, implying that the aggregation phenomena of ZnO nanoparticles are strongly quenched by the present of TPM stabilizers on the particle surfaces.

Monitoring the UV-vis absorption spectra of the ZnO colloidal solution is a useful and available tool to characterize the particle growth because the onset of absorption is associated with the particle size.[19–21,33] According to the experimental relationship between the average diameter (D) and the absorption shoulder ($\lambda_{1/2}$) of the ZnO nanoparticle colloids reported by Meulenkamp,[33] the particle sizes can be calculated based on the following calibrated equation.

$$1240/\lambda_{1/2} = 3.301 + 294.0/D^2 + 1.09/D \quad (1)$$

Thus, the average diameter of ZnO nanoparticles can be obtained and the results are shown in Fig. 3. Clearly, the size of unmodifed ZnO particles increased to about 6.7 nm after 10 days aging. In comparison, the particle sizes of the TPM-modified ZnO remained virtually unaltered from those of the fresh nanoparticles. After a period of 10 days at room

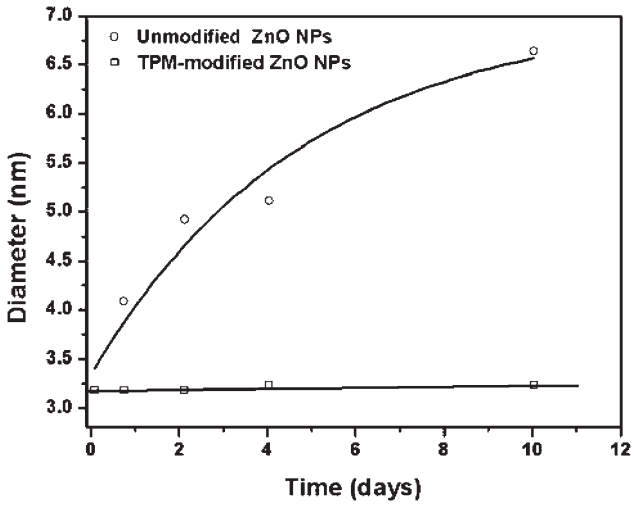

Fig. 3 Particle diameter *versus* aging time of the ZnO particles in ethanol.

temperature, the average diameters of TPM-modified particles was estimated to be still about 3.2 nm.

To further clarify the effect of TPM stabilizers on the aggregation state of nanoparticles, the crystal sizes of ZnO with different aging times were estimated by X-ray diffraction. Fig. 4 depicts typical powder X-ray diffraction patterns of unmodified and TPM-modified ZnO nanoparticles, taken for samples aged at 30 °C for 2 h, 3 days and 6 days after nanoparticle preparation. All diffraction peaks of these two profiles are consisted with typical wurtzite structure of bulk ZnO. Additionally, the aging time increase significantly influences the half-width of broadening peaks in the unmodified ZnO samples, as shown in Fig. 4a. In principle, the average ZnO crystal sizes (D) can be obtained by using Scherrer's equation, $D = 0.89\lambda/(\beta\cos\theta)$, where λ is the X-ray wavelength (1.54 Å), β is the half-width of the diffraction peak, and θ is the Bragg diffraction angle. By calculating the XRD diffraction peak broadening at (110), the average crystallite size of unmodified ZnO was estimated to be about 3.1 nm for 2 h, 4.3 nm for 3 days and 5.2 nm for 6 days. This result clearly indicates that the crystal growth process of the unmodified ZnO nanoparticles can easily occur even during aging at 30 °C, which agrees with previous results.[19] In contrast to the unmodified ZnO, the TPM-modified nanoparticle only slightly increased in crystal size from about 3.1 nm to 3.3 nm after aging for 6 days (Fig. 4b). All these results were consistent with our UV-vis spectral observations.

To confirm that the trimethoxy silane functionality of the TPM stabilizer capped/absorbed on the surface of ZnO nanoparticles, the purified powders were prepared through the "washing step" four times to ensure the removal of all of unreacted TPM stabilizer molecules. Fig. 5 shows the IR spectra of (a) unmodified ZnO and (b) TPM-modified ZnO nanoparticles. The absorption bands at 1579 cm^{-1} and 1415 cm^{-1} in both samples are assigned to the surface-absorbed carboxylate anions complexed with the zinc center,[20,21] indicating that the acetate group is chemisorbed on the ZnO nanoparticle surface. The addition of a stabilizing agent on the ZnO nanoparticle surfaces resulted in a different IR

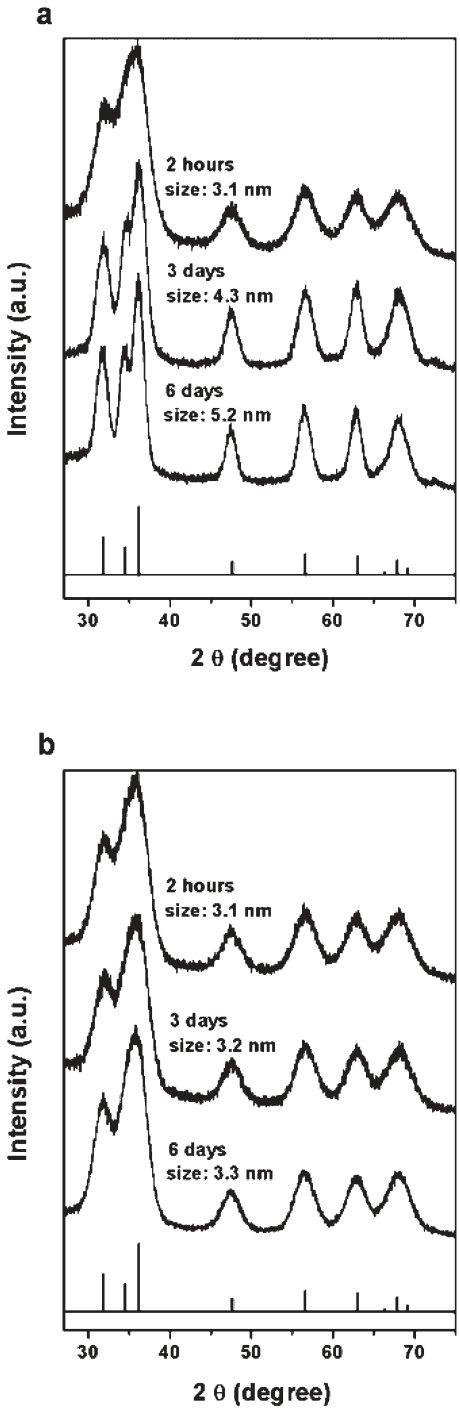

Fig. 4 Powder X-ray diffraction spectra of (a) umodified ZnO nanoparticles, (b) TPM-modified ZnO nanoparticles prepared with different aging times. The diffraction pattern of a wurtzite ZnO crystal from the JCPDS database is shown at the bottom for comparison.

spectrum (Fig. 5b). The characteristic absorption peaks of the TPM stabilizer are ascribed to the –OH stretching vibration at 3450 cm^{-1}, the C=O stretching vibration at 1704 cm^{-1}, the –SiOH stretching vibration at 880 cm^{-1},[37] and the peak at 1179 cm^{-1} was the characteristic peak of the Si–O–Si symmetrical stretching vibration.[38]

Purified powders of unmodified ZnO and TPM-modified ZnO nanoparticles were dispersed in DMSO-d_6 for ^{1}H NMR

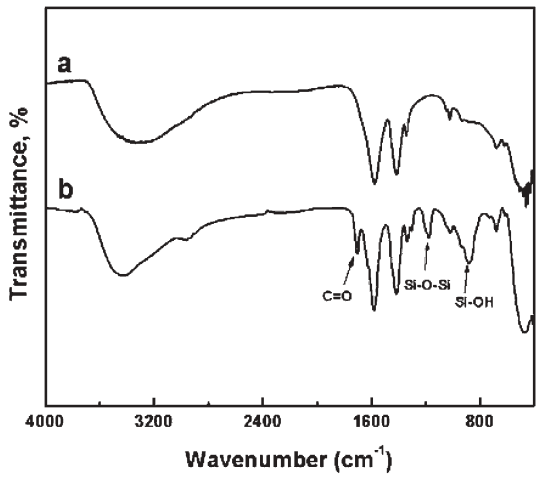

Fig. 5 FTIR spectra of the (a) unmodified ZnO nanoparticles and (b) TPM-modified ZnO nanoparticles.

measurements. Fig. 6 shows ^{1}H NMR of the pure TPM stabilizer, unmodified ZnO nanoparticles and TPM-modified ZnO nanoparticles. In the ^{1}H NMR spectrum of the TPM stabilizer (curve a), the resonance peaks at 6.02 and 5.65 ppm are assigned to the methylene protons (peaks H_1); and the three resonance peaks at 4.03, 1.66 and 0.62 ppm are assigned to the α-CH_2, β-CH_2 and γ-CH_2 protons (peaks H_3, H_4 and H_5) to methacrylate, respectively. The resonance peak at 1.87 ppm is assigned to be the methyl group near the methylene protons (peak H_2). The resonance peak at 3.47 ppm is caused by methyl protons of trimethoxysilane (peak H_6). In Fig. 6b, the spectrum of the unmodified ZnO nanoparticles, the peak at 1.72 ppm is attributed to the methyl proton of the acetate group, confirming the existence of the acetate group absorbed on the ZnO nanoparticle surfaces. Comparing ^{1}H NMR spectra of pure TPM stabilizer and TPM-modified ZnO nanoparticles (curves a and c), clearly the chemical shifts of peaks H_4 and H_5 are not observed and the chemical shifts of H_1, H_2, H_3 become significantly broadened in the TPM-modified ZnO nanoparticle sample. The broadening of the proton NMR spectrum is most likely due to inhomogeneities of the local chemical environment in the magnetic field. Usually, when protons are attached or absorbed at the surface of nanoparticles, the proton motion will become more restricted and the proton peak will become broader, or disappear.[39]

Base on the above FTIR and ^{1}H NMR observations, it is reasonable to conclude that the trimethoxysilyl groups of the TPM stabilizer absorbed on the as-prepared ZnO nanoparticle surface and yield a thin layer of organic silica nanonetwork *via* a hydrolysis–condensation reaction. We believe that the TPM stabilizer probably provided effective steric hindrance of the silica nanonetwork surrounding on the ZnO surfaces preventing colloid aggregation, thus leading to the excellent stability of ZnO nanoparticles in ethanol solution.

Photoluminescence and morphology of ZnO nanocomposites

As shown in Table 1, the photoluminescent properties (emission bands and quantum efficiencies) of ZnO

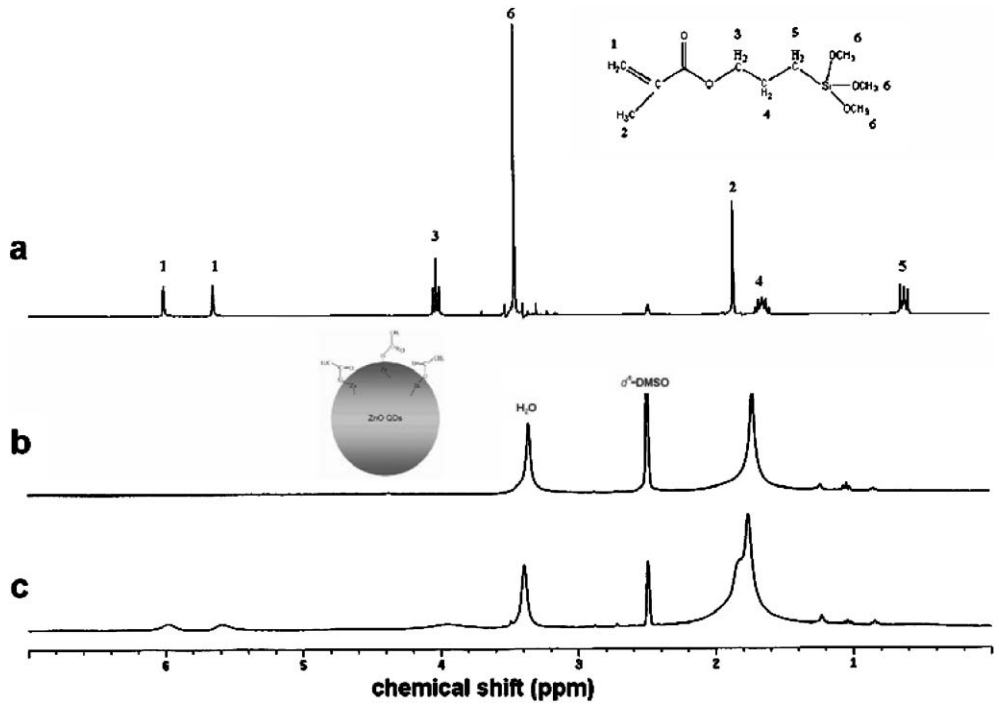

Fig. 6 ^{1}H NMR spectra of the (a) pure TPM stabilizer, (b) unmodified ZnO nanoparticles and (c) TPM-modified ZnO nanoparticles dispersed in DMSO-d_6.

nanoparticles in ethanol solution before and after addition of TPM stabilizer are similar, suggesting that the presence of such a silica network on the ZnO nanoparticle surfaces causes no significant fluorescence degradation or particle aggregation. Fig. 7 shows the PL spectra of the unmodified ZnO nanoparticle solutions and ZnO/PHEMA nanocomposites with an excitation wavelength at 325 nm. The TPM-modified ZnO nanocomposite with an average diameter of 3.2 nm is found to be remarkably similar to the initial unmodified nanoparticle solution, as shown in Fig. 7a. In contrast, the emission peak of the unmodified ZnO nanocomposite has a red shift. In Fig. 7b, the ZnO/PHEMA nanocomposite with an average diameter of 2.2 nm of TPM-modified ZnO gives a blue emission peak at 466 nm. Although the emission peaks of the 2.2 nm modified and unmodified ZnO nanocomposites all have red shifts, the TPM stabilizer obviously reduces the degree of shift. Since the emission bands of quantum-sized ZnO nanoparticles depend on the particle size,[19,21,23] the longer emission wavelength of ZnO/PHEMA nanocomposites without TPM stabilizer may contribute to the larger agglomerates and particle size increases in the course of thermal polymerization.

Due to the good miscibility and dispersibility of ZnO nanoparticles in HEMA monomer solution, stable optical transparent ZnO/PHEMA nanocomposites were readily obtained by common thermal polymerization. Fig. 8 shows photographs of the ZnO/PHEMA nanocomposites (*ca.* 1% wt of ZnO nanoparticles) under daylight and under UV light. Both TPM-modified and unmodified ZnO/PHEMA nanocomposites afford excellent optical transparency (Fig. 8a). Additionally, utilizing the precise size control and surface modification of ZnO nanoparticles into bulk nanocomposites allows adjustment of the emission colors from blue to orange (Fig. 8b–d). Moreover, the luminescent properties of ZnO/PHEMA nanocomposites display remarkable stability. For example, the emission peaks and intensities of these highly transparent nanocomposites were found to maintain similar values even after being aged over three months (see Table 1).

TEM was employed to examine the stability and dispersibility of the ZnO nanoparticles undergoing thermal

Table 1 Luminescence properties of ZnO NPs in solution and ZnO/PHEMA nanocomposites

	TPM-modified ZnO			Unmodified ZnO		
ZnO particle size/nm[a]	PL λ_{max} in ethanol solution/nm	PL λ_{max} in ZnO/PHEMA nanocomposite/nm	Φ^c (%)	PL λ_{max} in ethanol solution/nm	PL λ_{max} in ZnO/PHEMA nanocomposites/nm	Φ^c (%)
3.2	510	508 (510)[b]	6.2	506	530 (530)[b]	7.8
2.2	453	467 (468)[b]	10.5	447	515 (520)[b]	10.2

[a] NP diameters calculated from the shoulder of the absorption spectra. [b] Values in parentheses were recorded after three months of storage. [c] Fluorescence quantum yields of ZnO NPs in ethanol solution were obtained with quinine dye as a standard.

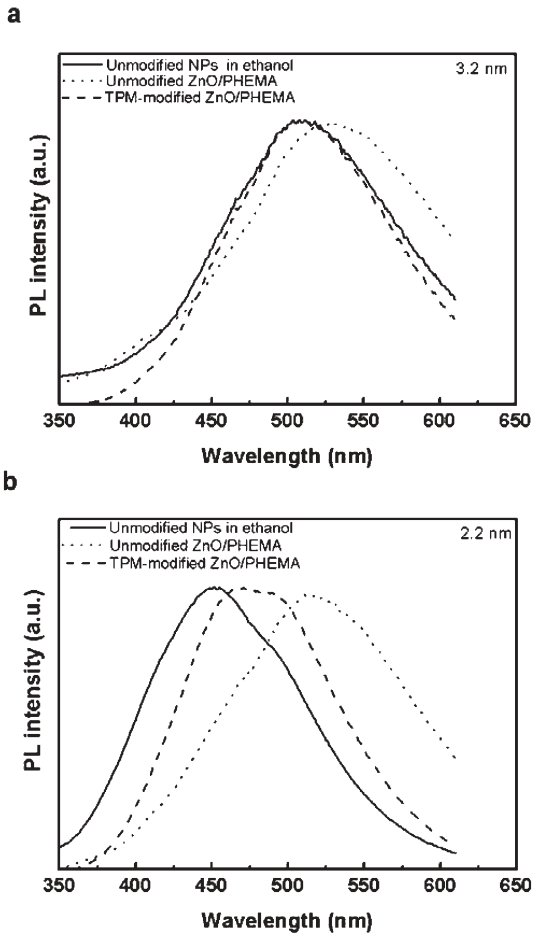

Fig. 7 Photoluminescence spectra of unmodified ZnO nanoparticles in ethanol solution, and modified and unmodified ZnO/PHEMA nanocomposites with different particle sizes: (a) 3.2 nm and (b) 2.2 nm.

polymerization at 70 °C and postheating procedure at 100 °C. As a representative example in Fig. 9a, large aggregate clusters in the unmodified ZnO/PHEMA nanocomposites were easily observed. In contrast, the 3.2 nm TPM-modified ZnO particles

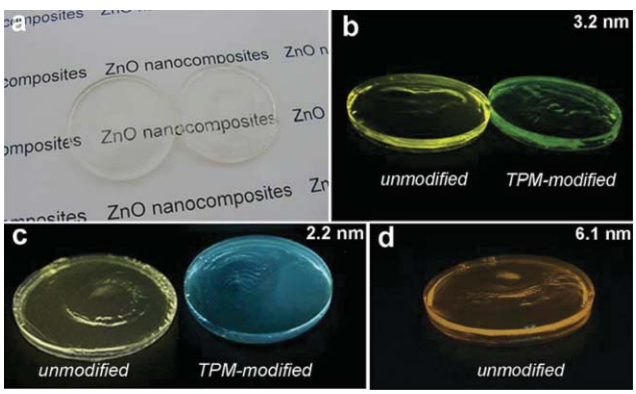

Fig. 8 Photographs of transparent ZnO/PHEMA nanocomposites with various particles sizes (a) under daylight and (b)–(d) under a UV lamp. Luminescence images of nanocomposites fabricated by ZnO particles with an average diameter of (b) 3.2 nm; (c) 2.2 nm; and (d) 6.1 nm, respectively.

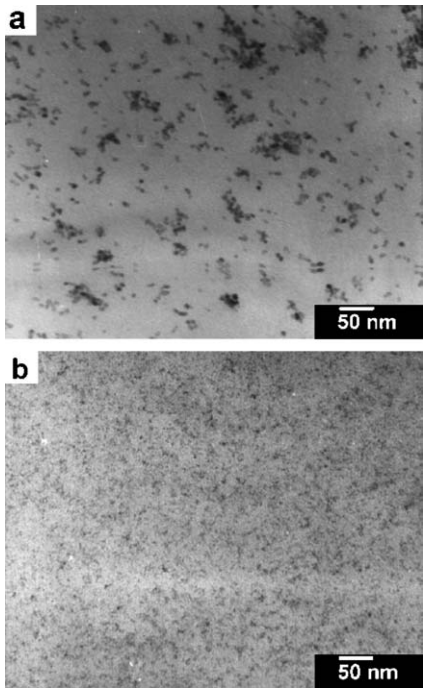

Fig. 9 Cross-section TEM images: (a) 6.1 nm unmodified ZnO particles in PHEMA matrix and (b) 3.2 nm TPM-modified ZnO particles in PHEMA matrix.

are well dispersed in the entire PHEMA matrix and the particle sizes are almost unchanged (Fig. 9b). These observations are consistent with the results of photoluminescence spectra, clearly supporting the idea that the TPM-surfaced modification really permits superior stability and dispersibility of ZnO nanoparticles into the polymer matrix compared to the unmodified ZnO nanoparticles, probably because of the covalent attachment between nanoparticles and polymers.

To further evaluate the influence of TPM on the dispersibility of ZnO nanoparticles in polymeric bulk, poly(methyl methacrylate) (PMMA) wasused to replace PHEMA in the preparation of ZnO nanocomposites. Fig. 10 is the photographs of ZnO/PMMA nanocomposites (a) under daylight and (b) under UV lamp with samples (I) 3.2 nm unmodified ZnO, (II) 3.2 nm TPM-modified ZnO and (III) 6.1 nm unmodified ZnO. Both unmodified ZnO samples I and III revealed particle precipitation and aggregation from the PMMA matrix, as the emission regions of samples in Fig. 10b. In contrast, sample

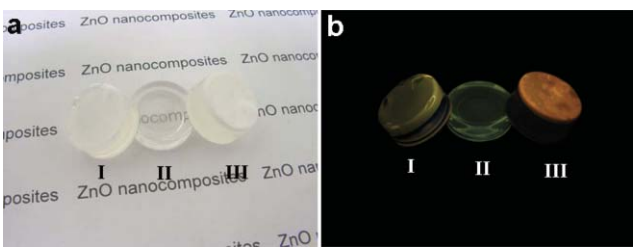

Fig. 10 Photographs of ZnO/PMMA nanocomposites (a) under daylight and (b) under a UV lamp with samples of (I) 3.2 nm unmodified ZnO, (II) 3.2 nm TPM-modified ZnO and (III) 6.1 nm unmodified ZnO.

(II) shows a relatively transparent and uniform appearance compared to the unmodified samples, indicating that the TPM stabilizer plays an important role in the optical quality of bulk nanocomposites.

Conclusion

In conclusion, the preparation of surface-modified ZnO nanoparticles with a layer of silica nanonetwork through a mild sol–gel route using TPM stabilizing agent has been demonstrated. The TPM stabilizer was shown to provide high dispersion stability of the ZnO nanoparticles in ethanol solution and preserve the size of nanoparticles near constant over long periods of time. The TPM-modified ZnO nanoparticles have better spatial separation than the unmodified ZnO nanoparticles in the nanohybrid film. Furthermore, the room temperature PL measurements also show that this surface-modified method can preserve the superior luminescence of ZnO nanoparticles in the nanohybrid films as well as in the initial nanoparticle solution. The surface modification method is believed to be an efficient approach to finely adjust the luminescent color and uniformity of bulk nanocomposites for developing novel electro-optical applications.

Acknowledgements

This research was supported by the National Science Council of the Republic of China under Grant NSC-92-2216-E-009-013 and Lee and MTI center in NCTU on photonic devices and modules project.

Chin-Hsien Hung and Wha-Tzong Whang*
Department of Materials Science and Engineering, National Chiao Tung University, Hsinchu, Taiwan 30049. E-mail: wtwhang@mail.nctu.edu.tw; Fax: 886-35-724727; Tel: 886-35-731873

References

1 V. L. Colvin, M. C. Schlamp and A. P. Alivisatos, *Nature*, 1994, **370**, 354–357.
2 A. P. Alivisatos, *Science*, 1996, **271**, 933–937.
3 M. H. Nayfeh, O. Akcakir, G. Belomonin, N. Barry, J. Therrien and E. Gratton, *Appl. Phys. Lett.*, 2000, **77**, 4086–4088.
4 C. Roland, V. Meunier, B. Larade and H. Guo, *Phys. Rev. B*, 2002, **66**, 35332.
5 M. Bruchez, M. Moronne, P. Gin, S. Weiss and A. P. Alivisatos, *Science*, 1998, **281**, 2013–2016.
6 Y. Yang, J. Huang, S. Liu and J. Shen, *J. Mater. Chem.*, 1997, **7**, 131–133.
7 J. Lee, V. C. Sundar, J. R. Heine, M. G. Bawendi and K. F. Jensen, *Adv. Mater.*, 2000, **12**, 1102–1105.
8 H. Zhang, Z. Cui, Y. Wang, K. Zhang, X. Ji, C. Lü, B. Yang and M. Gao, *Adv. Mater.*, 2003, **15**, 777–780.
9 S. C. Farmer and T. E. Patten, *Chem. Mater.*, 2001, **13**, 3920–3926.
10 N. Gaponik, D. V. Talapin, A. L. Rogach, A. Eychmuller and H. Weller, *Nano Lett.*, 2002, **2**, 803–806.
11 M. Moffitt, H. Vali and A. Eisenberg, *Chem. Mater.*, 1998, **10**, 1021–1028.
12 F. M. Pavel and R. A. Mackay, *Langmuir*, 2000, **16**, 8568–8574.
13 C. H. Chew, T. D. Li, L. H. Gan, C. H. Quek and L. M. Gan, *Langmuir*, 1998, **14**, 6068–6076.
14 M. Brust, M. Walker, D. Bethell, D. J. Schiffrin and R. Whyman, *J. Chem. Soc., Chem. Commun.*, 1994, 801–802.
15 C. L. Li and N. Murase, *Langmuir*, 2004, **20**, 1–4.
16 K. Hara, T. Horiguchi, T. Kinoshita, K. Sayama, H. Sugihara and H. Arakawa, *Sol. Energy Mater. Sol. Cells*, 2000, **64**, 115–134.
17 S. Bachir, C. Sandouly, J. Kossanyi and J. C. Ronfard-Haret, *J. Phys. Chem. Solids*, 1996, **57**, 1869–1879.
18 D. J. Goyal, C. Agashe, M. G. Takwale, V. G. Bhide, S. Mahamuni and S. K. Kulkarni, *J. Mater. Res.*, 1993, **8**, 1052–1056.
19 L. Spanhel and M. A. Anderson, *J. Am. Chem. Soc.*, 1991, **113**, 2826–2833.
20 S. Monticone, R. Tufeu and A. V. Kanaev, *J. Phys. Chem. B*, 1998, **102**, 2854–2862.
21 S. Sakohara, M. Ishida and M. A. Anderson, *J. Phys. Chem. B*, 1998, **102**, 10169–10175.
22 H.-M Xiong, X. Zhao and J.-S. Chen, *J. Phys. Chem. B*, 2001, **105**, 10169–10174.
23 E. M. Wong and P. C. Searson, *Appl. Phys. Lett.*, 1999, **74**, 2939–2941.
24 N. S. Pesika, Z. Hu, K. J. Stebe and P. C. Searson, *J. Phys. Chem. B*, 2002, **106**, 6985–6990.
25 L. Guo, S. Yang, C. Yang, P. Yu, J. Wang, W. Ge and G. K. L. Wong, *Appl. Phys. Lett.*, 2000, **76**, 2901–2903.
26 G. Rodriguez-Gattorno, P. Santiago-Jacinto, L. Rendon-Vazquez, J. Nemeth, I. Dekany and D. Diaz, *J. Phys. Chem. B*, 2003, **107**, 12597–12604.
27 M. Shim and P. Guyot-Sionnest, *J. Am. Chem. Soc.*, 2001, **123**, 11651–11654.
28 P. D. Cozzoli, M. L. Curri, A. Agostiano, G. Leo and M. Lomascolo, *J. Phys. Chem. B*, 2003, **107**, 4756–4762.
29 J. Hambrock, S. Rabe, K. Merz, A. Birkner, A. Wohlfart, R. A. Fischer and M. Driess, *J. Mater. Chem.*, 2003, **13**, 1731–1736.
30 Mikrajuddin, F. Iskandar, K. Okuyama and F. G. Shi, *J. Appl. Phys.*, 2001, **89**, 6431–6434.
31 M. Abdullah, I. W. Lenggoro, K. Okuyama and F. G. Shi, *J. Phys. Chem. B*, 2003, **107**, 1957–1961.
32 P. Hoyer, R. Eichberger and H. Weller, *Ber. Bunsen-Ges. Phys. Chem.*, 1993, **97**, 630–635.
33 E. A. Meulenkamp, *J. Phys. Chem. B*, 1998, **102**, 5566–5572.
34 W. R. Dawson and M. W. Windsor, *J. Phys. Chem.*, 1968, **72**, 3251–3260.
35 M. Haase, H. Weller and A. Henglein, *J. Phys. Chem.*, 1988, **92**, 482–487.
36 U. Koch, A. Fojtik, H. Weller and A. Henglein, *Chem. Phys. Lett.*, 1985, **122**, 507–510.
37 M. Nandi, J. A. Coklin, L. Salvati and A. Sen, *Chem. Mater.*, 1991, **3**, 201–206.
38 X.-Y. Shang, Z.-K. Zhu, J. Yin and X.-D. Ma, *Chem. Mater.*, 2002, **14**, 71–77.
39 O. Kohlmann, W. E. Steinmetz, X.-A. Mao, W. P. Wuelfing, A. C. Templeton, R. W. Murray and C. S. Johnson, Jr., *J. Phys. Chem. B*, 2001, **105**, 8801–8809.

